

**$^{10}\text{Be}$ ,  $^{26}\text{Al}$ , AND  $^{36}\text{Cl}$  IN IRON METEORITES: IMPLICATIONS FOR OSMIUM ISOTOPE SYSTEMATICS.** N. Shankar<sup>1,3</sup>, G. Ruge<sup>4</sup>, T. Faestermann<sup>4</sup>, G. Korschinek<sup>4</sup>, C. C. Swisher III<sup>2,3</sup>, B. Turrin<sup>2,3</sup>, G. F. Herzog<sup>1,3</sup>, and R. J. Walker<sup>5</sup>, <sup>1</sup>Dept. Chem. & Chem. Biol. <nirmalas@eden.rutgers.edu>, <sup>2</sup>Dept. Earth & Planet. Sci., <sup>3</sup>Rutgers Univ., Piscataway, NJ 08854, <sup>4</sup>Fakultät für Physik, Technische Universität Munchen, Germany, <sup>5</sup>Dept. Geology, Univ. Maryland, College Park, MD 20742.

**Introduction:** Cosmic ray exposure (CRE) of iron meteorites may lead to unwanted but correctable changes in the isotope ratios needed to calculate Re/Os and W/Hf ages and to identify isotopic anomalies [1,2,3]. The size of the effects depends on the CRE history, i.e., on meteoroid shielding and the duration of exposure. We report the activities of the cosmogenic radionuclides (CRN)  $^{10}\text{Be}$  ( $t_{1/2} = 1.39$  Ma),  $^{26}\text{Al}$  ( $t_{1/2} = 0.7$  Ma), and  $^{36}\text{Cl}$  ( $t_{1/2} = 0.3$  Ma) in eight iron meteorites for which highly-precise Os isotope ratios have been measured [1]. From the results we infer terrestrial ages and shielding conditions for these samples and estimate attendant changes in the  $^{190}\text{Os}/^{188}\text{Os}$  and  $^{189}\text{Os}/^{188}\text{Os}$  ratios.

**Experimental methods:** Meteorites thought to have had simple CRE histories were chosen for study (Table 1). One-gram aliquots of samples previously analyzed for Os were cut into two pieces (~0.2 g and ~0.8 g). The 0.2-g sample was dissolved in 2M  $\text{HNO}_3$  along with carriers for Be (1.8 mg), Al (1.8 mg), and Cl (5 mg). Once chemically separated,  $\text{BeO}$ ,  $\text{Al}_2\text{O}_3$ , and  $\text{AgCl}$ , were analyzed at Purdue University by accelerator mass spectrometry. The solutions containing Ni were reserved for measurements of  $^{59}\text{Ni}$  and the 0.8-g sample for noble gas analysis.

**Results:** Our measurements (Table 1) generally agree with previously published work. The anomalies (italicized) are discussed with production rates, below. Activities (dpm/kg) for all meteorites except Charlotte and Grant (Table 1) fall below the ranges of values commonly reported for irons, namely,  $3 \leq ^{10}\text{Be} \leq 6$ ,  $2 \leq ^{26}\text{Al} \leq 5$ , and  $14 \leq ^{36}\text{Cl} \leq 23$  [4,5,6].

**Production rates - Terrestrial ages** (Table 2) were calculated from  $^{36}\text{Cl}/^{10}\text{Be}$  ratios [5, 12, 13].

CRN activities corrected to the time of fall (ToF) should equal production rates given the long CRE ages (Table 2) for these meteorites [14]. ToF activities for Bennett County, Charlotte, Grant, and Tlacotepec are in or close to the normal range. Unsurprisingly, lower values for the large meteorites Gibeon, Henbury, and Hoba signal heavy shielding. The ToF activities correlate well (Figure 1): The average ratios,  $^{10}\text{Be}/^{26}\text{Al} = 1.2 \pm 0.2$  and  $^{36}\text{Cl}/^{26}\text{Al} = 6.6 \pm 0.7$ , which differ slightly from the slopes of the lines in Figure 1, may be compared to published values of  $^{10}\text{Be}/^{26}\text{Al}$  of  $1.3 \pm 0.1$  [5] and  $1.4 \pm 0.2$  [6] and  $^{36}\text{Cl}/^{26}\text{Al} = 6.9 \pm 0.1$  [5]. The measured ratios for Tlacotepec, CoGH, and Bennett County deviate from

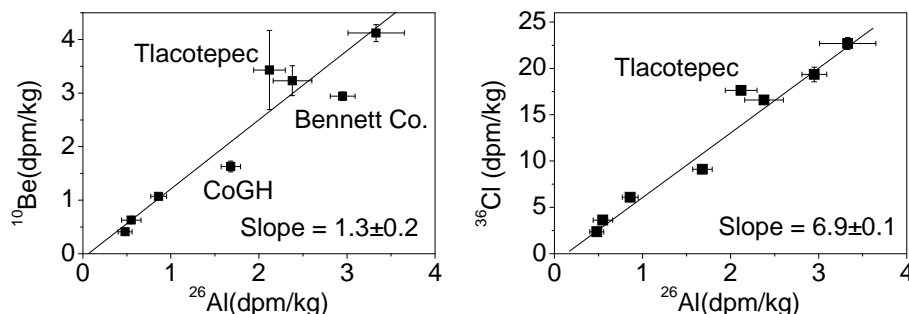


Figure 1: Correlation of CRN activities

Table 1: Activities (dpm/kg)

| Meteorite    | $^{10}\text{Be}$     | $^{26}\text{Al}$     | $^{36}\text{Cl}$     |
|--------------|----------------------|----------------------|----------------------|
| Bennett Co.  | $2.68 \pm 0.08$      | $2.82 \pm 0.13$      | $17.31 \pm 0.71$     |
|              | $3.86 \pm 0.19^6$    | $2.97 \pm 0.18^6$    | $18.99 \pm 0.49^6$   |
| Cape of Good | $1.49 \pm 0.10$      | $1.42 \pm 0.09$      | $6.13 \pm 0.23$      |
| Hope (CoGH)  | $2.13 \pm 0.11^6$    | $1.46 \pm 0.09^6$    |                      |
| Charlotte    | $4.12 \pm 0.17$      | $3.33 \pm 0.32$      | $22.68 \pm 0.65$     |
|              | $4.71 \pm 0.40^4$    | $5.07 \pm 0.20^4$    | $25.40 \pm 1.00^7$   |
|              | $6.00 \pm 0.30^6$    | $4.20 \pm 0.25^6$    |                      |
| Gibeon       | $0.58 \pm 0.02$      | $0.48 \pm 0.10$      | $2.59 \pm 0.10$      |
|              | $0.58 \pm 0.01^8$    | $< 0.7^9$            | $2.87 \pm 0.14^8$    |
| Grant K-306  | $3.16 \pm 0.27$      | $2.28 \pm 0.21$      | $15.04 \pm 0.38$     |
|              | $3.10 \pm 0.16^6$    | $2.38 \pm 0.14^6$    |                      |
| Henbury      | $0.98 \pm 0.04$      | $0.74 \pm 0.09$      | $4.32 \pm 0.22$      |
|              | $1.43 \pm 0.10^{10}$ | $0.95 \pm 0.09^{10}$ |                      |
| Hoba         | $0.36 \pm 0.01$      | $0.36 \pm 0.08$      | $1.35 \pm 0.06$      |
|              | $0.68 \pm 0.14^{11}$ | $0.27 \pm 0.10^{11}$ | $1.56 \pm 0.08^{11}$ |
| Tlacotepec   | $2.82 \pm 0.74$      | $1.48 \pm 0.15$      | $7.56 \pm 0.27$      |
|              | $3.06 \pm 0.15^6$    | $3.04 \pm 0.15^4$    |                      |
|              |                      | $1.74 \pm 0.10^6$    |                      |

these averages; unknown errors in the italicized data in Table 1 offer the simplest explanation for the differences, but we have no experimental reasons for rejecting these data.

**CRE ages:** To calculate the shielding-corrected CRE ages we need cosmogenic  $^{21}\text{Ne}$  and  $^{36}\text{Ar}$  concentrations at the depths of our samples. To estimate  $^{21}\text{Ne}_{\text{cos}}$  and  $^{36}\text{Ar}_{\text{cos}}$ , we plotted them vs.  $^4\text{He}/^{21}\text{Ne}$  using all the available literature values [16]. The shielding parameters,  $^4\text{He}/^{21}\text{Ne}$ , for our samples were estimated from the relation  $^{10}\text{Be}(\text{ToF, dpm/kg}) = (8.9 \pm 0.8) - (0.18 \pm 0.004) \times ^4\text{He}/^{21}\text{Ne}$  [4]. Results are given in Table 2. We then read from the plots the  $^{21}\text{Ne}_{\text{cos}}$  and  $^{36}\text{Ar}_{\text{cos}}$  concentrations corresponding to our estimated  $^4\text{He}/^{21}\text{Ne}$  ratios. In calculating CRE ages, we took for the production rate ratios (atom/atom)  $P(^{10}\text{Be})/P(^{21}\text{Ne}) = 0.55$ ,  $P(^{26}\text{Al})/P(^{21}\text{Ne}) = 0.38$ , and  $P(^{36}\text{Cl})/P(^{36}\text{Ar}) = 0.82$  [5].

**Shielding depths and radii:** The radii for the meteorites were taken from [14]. The approximate depths at which the radionuclides were produced were estimated from the ToF CRN activities and the model of [15] (Table 2).

**Prediction of  $^{59}\text{Ni}$  (dpm/kg), neutron fluence,  $\epsilon^{189}$ , and  $\epsilon^{189}$ :** A  $^{59}\text{Ni}$  (dpm/kg) depth profile has been measured for Canyon Diablo [17], a very large iron meteorite. We used this profile to estimate the  $^{59}\text{Ni}$  activities expected for Hoba and Gibeon.  $^{59}\text{Ni}$  production rate profile calculations are not yet available for smaller irons, but they are for ordinary chondrites [18]. Using the latter profiles and the depths of Table 2, we estimated the  $^{59}\text{Ni}$  (dpm/kg) activities, and hence production rates,  $P_{59}$ , expected for the other irons of Table 2. We calculated thermal neutron fluxes,  $\phi$  neutron  $\text{cm}^{-2} \text{s}^{-1}$ , from the relation  $P_{59} =$

$P_{59}$  production rate profile calculations are not yet available for smaller irons, but they are for ordinary chondrites [18]. Using the latter profiles and the depths of Table 2, we estimated the  $^{59}\text{Ni}$  (dpm/kg) activities, and hence production rates,  $P_{59}$ , expected for the other irons of Table 2. We calculated thermal neutron fluxes,  $\phi$  neutron  $\text{cm}^{-2} \text{s}^{-1}$ , from the relation  $P_{59} =$

$\phi\sigma_{58}N_{58}$  with  $\sigma_{58}=4.6$  b [19] and the known Ni concentrations [19]. Multiplication of  $\phi$  by the CRE age gives the fluence,  $\Phi$ , needed to estimate  $\varepsilon^x=\varepsilon(^x\text{Os}/^{188}\text{Os})$ . Specifically, the changes in the atom concentrations,  $N$ , were obtained from the approximate relations  $\Delta^{190}N = {}^{189}N_0\sigma_{189}\Phi$ ;  $\Delta^{189}N = {}^{188}N_0\sigma_{188}\Phi - {}^{189}N_0\sigma_{189}\Phi$ ; and  $\Delta^{188}N = {}^{187}N_0\sigma_{187}\Phi - {}^{188}N_0\sigma_{188}\Phi \sim 0$ ; here subscript 0 denotes initial with isotope ratios from [19]. The value of  $\varepsilon$  was calculated using its definition.

$$\varepsilon^y = \left[ \frac{\left( \frac{{}^y\text{Os}_n + {}^y\text{Os}_0}{{}^{188}\text{Os}_n + {}^{188}\text{Os}_0} \right)}{\frac{{}^y\text{Os}_0}{{}^{188}\text{Os}_0}} + 1 \right] \times 10,000; y = 189, 190$$

The neutron cross sections ( $\sigma$ , barn = thermal plus resonance integral) for  $\text{Os}_{188}$  and  $\text{Os}_{189}$  were taken as 159 and 709, respectively [19]. Values of  $\varepsilon^{189}\text{Os}$  and  $\varepsilon^{190}\text{Os}$  calculated with  $T_{10}$  are given in Table 2; use of  $T_{40}$  would increase these values by about 40%. Compared to our calculated values, measured values for  $\varepsilon^{189}\text{Os}$  and  $\varepsilon^{190}\text{Os}$  [1] are 13 $\times$  higher for Tlacotepec and 3-6 $\times$  higher for the other irons. Our calculations assume that the fluence of low-energy neutrons is completely thermalized. Detailed modeling calculations [20] show that for radii  $< \sim 50$  cm, this is not the case and that resonance absorption effects may strongly influence capture rates. Although  ${}^{189,190}\varepsilon_{\text{measured}}$  and  ${}^{189,190}\varepsilon_{\text{calculated}}$  differ, they follow similar trends, with absolute magnitudes increasing in the order Charlotte < Gibeon < Grant < Hoba < Tlacotepec; the only exception is CoGH. No calculations were possible for Bennett Co. or Henbury. Plots of  ${}^{190}\varepsilon$  vs.  ${}^{189}\varepsilon$  for measured

and predicted values have similar slopes,  $-0.63 \pm 0.05$  and  $-0.90 \pm 0.01$ , respectively. Measurements of  ${}^{59}\text{Ni}$  (dpm/kg) and more detailed modeling calculations are required to reconcile predictions with observations.

**Conclusion:** From measured  ${}^{10}\text{Be}$ ,  ${}^{26}\text{Al}$ , and  ${}^{36}\text{Cl}$  activities and published data we inferred the shielding conditions for eight samples from iron meteorites. From these results and CRE ages, we estimated the likely effects on osmium isotope systematics. The estimates agree marginally within errors for Hoba and Gibeon in which thermalization of neutrons can be expected, but are too small by a factor of up to 13 for smaller irons.

**References:** [1] Walker R. et al. (2010) *LPS*, 1324.pdf. [2] Leya I. et al. (2000) *EPSL*, 175, 1-12. [3] Huang S. and Humayun M. (2008) *LPSC*, 1168.pdf. [4] Aylmer D. et al. (1985). *EPSL*, 88, 107-118. [5] Lavielle B. et al. (1999) *EPSL*, 170, 93-104. [6] Xue S. et al. (1995) *EPSL*, 136, 397-406. [7] Vilcsek E. and Wänke H. (1963) in *Radioactive Dating*, 381-393. [8] Honda M. et al. (2009) *J. Phys. Soc. Japan*, 78, 12-17. [9] Hampel W. and Schaeffer O. A. (1979) *EPSL*, 42, 348- 358. [10] Nagai H. et al. (1987) *NIM*, B29, 266-270. [11] McCorkell R. H. et al. (1968) *Meteoritics*, 4, 113-122. [12] Chang C. and Wänke H. (1969) in *Meteorite Research*, 397-406. [13] Nishiizumi K. et al. (1997) *M&PS*, 32, A100. [14] Voshage H. and Feldmann H. (1979) *EPSL*, 45, 293-308. [15] Ammon K. et al. (2009), *M&PS*, 44, 485-503. [16] Schultz L. and Kruse H. (1989), *Meteoritics*, 24, 155-172 [17] Schnabel C. et al. (1999), *Science*, 285, 85-88. [18] Spergel M. S. et al. (1986) *LPI*, 71-72. [19] Mughabghab S. F. (1984) *Neutron Resonance Parameters and Thermal Cross Sections*, Academic Press, NY. [20] Leya I. *Pers. comm.*

**Table 2:** CRE ages and measured and calculated values of  $\varepsilon^{189}\text{Os}/^{188}\text{Os}$  and  $\varepsilon^{190}\text{Os}/^{188}\text{Os}$ .

| Meteorite                                      | Bennett Co.<br>(IIAB) | CoGH<br>(IVB)    | Charlotte<br>(IVA) | Gibeon<br>(IVA)  | Grant<br>(IIIAB) | Henbury<br>(IIIAB) | Hoba<br>(IVB)    | Tlacotepec<br>(IVB) |
|--|-----------------------|------------------|--------------------|------------------|------------------|--------------------|------------------|---------------------|
| Mass (T)                                       | 0.089                 | 0.136            | 4                  | 26               | 0.48             | 2                  | 60               | 0.071               |
| $T_{\text{terr}}$ (ka)                         | 48 $\pm$ 32*          | 171 $\pm$ 41     | Fall               | 148 $\pm$ 28     | 43 $\pm$ 49      | 148 $\pm$ 33       | 244 $\pm$ 30     | 366 $\pm$ 134       |
| ${}^{10}\text{Be}$ (dpm/kg)                    | 2.9 $\pm$ 0.1         | 1.6 $\pm$ 0.1    | 4.1 $\pm$ 0.2      | 0.63 $\pm$ 0.02  | 3.2 $\pm$ 0.3    | 1.07 $\pm$ 0.04    | 0.41 $\pm$ 0.02  | 3.4 $\pm$ 0.7       |
| ${}^4\text{He}/{}^{21}\text{Ne}$               | 331 $\pm$ 63          | 404 $\pm$ 76     | 265 $\pm$ 50       | 460 $\pm$ 87     | 315 $\pm$ 60     | 435 $\pm$ 82       | 472 $\pm$ 89     | 304 $\pm$ 58        |
| Radius (cm)                                    |                       | 122              | 25                 | Large            | 39               |                    | Large            | 45                  |
| Depth (cm)                                     | 10                    | 40               | 10                 | 60-80            | 2                | 50                 | 80               | 15                  |
| $T_{10\text{Be}/21\text{Ne}}$ (Ma)             |                       | 434 $\pm$ 28     | 274 $\pm$ 30       | 81 $\pm$ 5       | 484 $\pm$ 43     | 979 $\pm$ 38       | 207 $\pm$ 6      | 553 $\pm$ 119       |
| $T_{26\text{Al}/21\text{Ne}}$ (Ma)             |                       | 291 $\pm$ 20     | 234 $\pm$ 23       | 63 $\pm$ 12      | 455 $\pm$ 45     | 840 $\pm$ 89       | 122 $\pm$ 21     | 617 $\pm$ 53        |
| $T_{36\text{Cl}/36\text{Ar}}$ (Ma)             |                       | 457 $\pm$ 15     | 228 $\pm$ 8        | 82 $\pm$ 3       | 442 $\pm$ 14     | 827 $\pm$ 48       | 195 $\pm$ 7      | 535 $\pm$ 15        |
| $T_{40\text{K}/\text{K}}^{14}$ (Ma)            |                       | 775 $\pm$ 70     | 365 $\pm$ 80       |                  | 695 $\pm$ 65     |                    | 340 $\pm$ 110    | 945 $\pm$ 55        |
| ${}^{59}\text{Ni}$ (dpm/[kg Ni])               |                       | 845              | 282                | 1408             | 282              |                    | 845              | 563                 |
| $\Phi$ (neutron $\text{cm}^{-2}$ , $10^{15}$ ) |                       | 6.02             | 1.26               | 1.87             | 2.23             |                    | 2.86             | 5.10                |
| $\varepsilon^{189}$ this work                  |                       | -0.032           | -0.007             | -0.010           | -0.012           |                    | -0.015           | -0.027              |
| $\varepsilon^{189}$ [1]                        | -0.08 $\pm$ 0.12      | -0.22 $\pm$ 0.18 | 0.01 $\pm$ 0.05    | 0.01 $\pm$ 0.08  |                  | -0.23 $\pm$ 0.09   | -0.08 $\pm$ 0.05 | -0.54 $\pm$ 0.07    |
| $\varepsilon^{190}$ this work                  |                       | 0.029            | 0.006              | 0.009            | 0.011            |                    | 0.014            | 0.024               |
| $\varepsilon^{190}$ [1]                        | 0.06 $\pm$ 0.13       | 0.15 $\pm$ 0.10  | -0.02 $\pm$ 0.12   | -0.04 $\pm$ 0.15 |                  | 0.17 $\pm$ 0.16    | 0.07 $\pm$ 0.12  | 0.32 $\pm$ 0.11     |

$t_{10} = 511 \times 0.55 \times \frac{{}^{21}\text{Ne}}{{}^{10}\text{Be}}$ ,  $t_{26} = 511 \times 0.38 \times \frac{{}^{21}\text{Ne}}{{}^{26}\text{Al}}$ ,  $t_{36} = 511 \times 0.82 \times \frac{{}^{36}\text{Ar}}{{}^{36}\text{Cl}}$ ; Activities (dpm/kg);  ${}^{21}\text{Ne}$ ,  ${}^{36}\text{Ar}$  ( $10^{-8}$   $\text{cm}^3$  STP  $\text{g}^{-1}$ ).

Data in italics considered suspect. \*Calculated using  ${}^{10}\text{Be}$  data from literature [6]